IEEE Access
Multidisciplinary | Rapid Review | Open Access Journal

Received July 22, 2017, accepted August 7, 2017, date of publication August 14, 2017, date of current version October 12, 2017.

Digital Object Identifier 10.1109/ACCESS.2017.2739205

An Electret-Based Angular Electrostatic Energy Harvester for Battery-Less Cardiac and Neural Implants

SUHAIB AHMED, (Student Member, IEEE), AND VIPAN KAKKAR, (Senior Member, IEEE)
Department of Electronics and Communication Engineering, Shri Mata Vaishno Devi University, Katra 182320, India
Corresponding author: Suhaib Ahmed (sabatt@outlook.com)

ABSTRACT The implantable microsystems are conventionally powered using batteries that have limited life-span and bio-compatibility issues. Hence, energy harvesting as an alternate and continuous power source in miniaturized implantable medical devices, especially cardiac and neural implants, has been investigated in this paper. An electret-based electrostatic energy harvester has been proposed with angular electrode structures along with a switching converter circuit to harvest maximum possible energy. The proposed harvester incorporates the properties of both area-overlap and gap closing topologies to achieve larger capacitance variation with respect to displacement, as is observed in the results. The maximum power that can be scavenged from the proposed harvester with an active surface area of 2.5 $\times$ 3.5 mm^2 and volume 0.4375 mm^3 at maximum displacement is 9.6 μW; along with a maximum power per unit surface area of 109.71 μW/cm^2, which is within the advised limit of power density for *in vivo* implantable applications. Hence, the proposed electrostatic harvester can be used as a power source for cardiac and neural implants.

INDEX TERMS Cardiac implant, electret, electrostatic conversion, energy harvesting, neural implant.

I. INTRODUCTION

The recent developments in the field of electronics, micro-electro-mechanical systems (MEMS) and wireless technology has enabled the intensive integration of system-on-chip and low power electronics, which has led to a very fast growth in the medical device industry and has recorded a great research activity over the past decade [4]–[7]. One such development has been in wearable and implantable medical devices (IMDs), such as cardiac and neural implants, which has improved the healthcare facilities being provided to patients.

To ensure the proper functioning of the IMDs, a permanent and efficient power source is required. Since the introduction of first cardiac implant pacemaker in 1972 [10], various batteries have been designed and used in IMDs [11]–[15]. Lithium-based batteries, owing to their high energy density and small size, have been commonly used in the implants [13], [17]. However, these batteries have a limited life span, which requires the replacement of these batteries by surgery. Hence, alternative energy sources are required to power these IMDs. Energy harvesting is one such concept which can address the problems of life span, energy density, small size and biocompatibility.

Energy harvesting is the process of scavenging out energy from different sources in the ambient environment. Various harvesters are being proposed to harvest energy for implantable devices. The form of energy used by the harvester to scavenge the power, defines the type of energy harvesting. There are four main ambient energy sources available viz., mechanical energy (vibrations, deformations) [18]–[20], thermal energy (temperature variations and gradients) [21]–[23], radiant energy (sun, IR, RF) [24], [25] and biochemical (bio-fuel cells) [26]–[28]. A comparison of the power densities of these different energy sources is presented in Fig. 1 [1].

It is observed that a radiant energy source, such as the Sun, is the most powerful energy source. However, given the application in concern, radiant energy harvesting is not possible in implants and same is the case with thermal sources. Bio-fuel cells can be considered, however, they have lower power densities compared to vibrational mechanical sources. Although, the power density of the vibrational source is only 1-100 μW, it is still sufficient for application in cardiac and neural implants.

The rest of the paper has been organized as follows. In section II, vibration based energy harvesters and its types

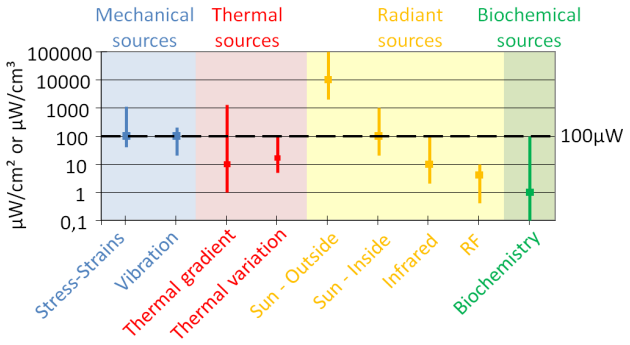

FIGURE 1. Comparison of power densities of different ambient energy sources [1].

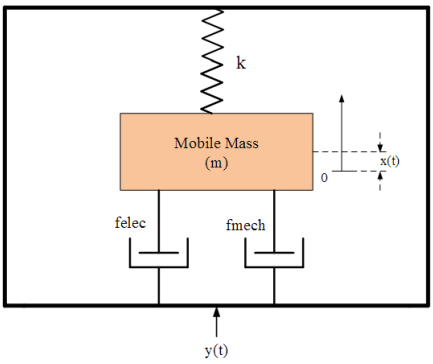

FIGURE 3. Vibration energy harvester equivalent model.

are discussed, followed by the discussion on electrostatic harvesters and its types in section III.

Different topologies of the electrostatic harvesters are presented in section IV. The proposed electret-based electrostatic harvester with angular electrodes is presented in section V. Finally, the simulation results and discussions are presented in section VI followed by the conclusion in section VII.

II. VIBRATION ENERGY HARVESTING

Vibrations are an effective source of mechanical energy present in the human body, and this energy can be scavenged using the vibration energy harvester to power the implantable microsystems. It follows a two-step conversion [1], [29] shown in Fig. 2. At first the vibrations from the ambient conditions are converted into relative motion using a mass-spring system, and then this relative motion is converted into electricity by the mechanical to electrical converter. The mass-spring system amplifies the relative motion low level amplitude, and usually generates maximum power at resonant frequency.

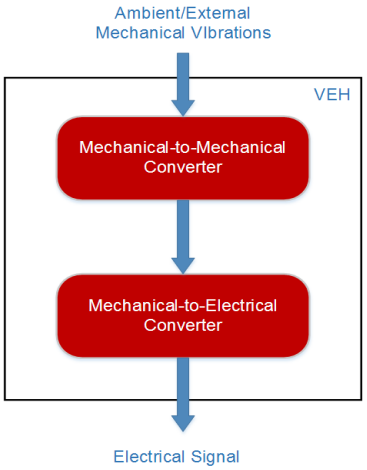

FIGURE 2. Vibration energy harvesting (VEH) conversion process.

The vibration based energy harvesters can be modelled as shown in Fig. 3. It consists of a movable mass (m) suspended by a spring, with spring constant (k), to the fixed frame and damped by electromechanical force (f_{elec}) and friction force (f_{mec}). Electricity (f_{elec}) is scavenged from the kinetic energy induced due to relative motion $x(t) = Xsin(\omega t + \Phi)$ upon subjection of external vibration $y(t) = Ysin(\omega t)$ on the harvester. The electromechanical and friction forces [1] can be modelled as

$$f_{elec} = b_e \frac{dx(t)}{dt} \tag{1}$$

$$f_{mec} = b_m \frac{dx(t)}{dt} \tag{2}$$

Where, b_e and b_m are the electrical and mechanical damping coefficients respectively. The relative motion can thus be modelled as a differential equations [1] governed by the Newton's second law as

$$m\frac{d^2x(t)}{dt^2} + m\frac{d^2y(t)}{dt^2} + kx(t) + f_{mec} + f_{elec} = 0 \tag{3}$$

This can be further simplified as

$$\frac{d^2x(t)}{dt^2} + \frac{\omega_0}{Q_m} + \omega_0^2 x(t) + \frac{f_{elec}}{m} = -\frac{d^2y(t)}{dt^2} \tag{4}$$

Where, $\omega_0 = \sqrt{k/m}$ is the angular frequency and $Q_m = m\omega_0/b_m$ is the quality factor. The maximum mechanical power that can be scavenged is then given by [1], [30]

$$P = \frac{mY^2\omega_0^3 Q_m}{8} \tag{5}$$

In order to extract this mechanical energy, a mechanical-to-electrical converter is required. Generally there are three such converters viz., piezoelectric, electrostatic and electromagnetic converters.

A. PIEZOELECTRIC CONVERTER

The ability of piezoelectric materials to produce charges under applied stress/strain (as shown in fig. 4) forms the principle in piezoelectric energy harvesting [29], [31]. The piezoelectric property produces electrical energy from mechanical energy (energy due to relative motion). When an electric field is created upon mechanical deformation, the effect is called as the direct piezoelectric effect. On the other hand, when an applied electric field causes mechanical deformation, it is

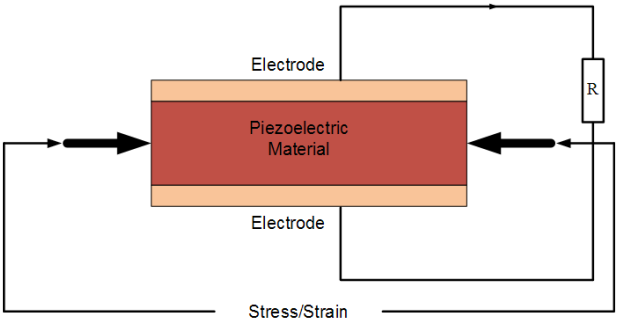

FIGURE 4. Piezoelectric mechanical-to-electrical converter concept model.

called an indirect piezoelectric effect. In energy harvesting, the concept of direct piezoelectric effect is used to convert mechanical energy into electrical. The materials such as puttered zinc oxide, quartz, lead zirconate titanate (PZT), and polyvinylidenefluoride (PVDF) [29], [32] exhibit this effect

B. ELECTROSTATIC CONVERTER

This converter uses a variable capacitor structure, as shown in Fig. 5, to generate charges whenever relative motion is induced due to external vibrations. The electrostatic converter uses the electrostatic interactions [29], [33] between two conductor plates of the capacitor which are electrically isolated by air, vacuum or any dielectric material. Whenever there is a relative motion between the plates due to external vibration, the harvester operates against the electrostatic attraction, and transduces the mechanical energy into electrical charges that are stored on the conductor plates.

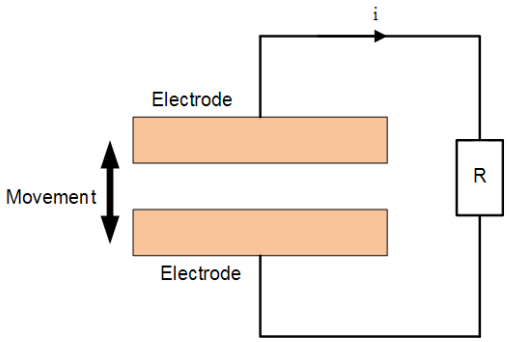

FIGURE 5. Electrostatic mechanical-to-electrical converter concept model.

C. ELECTROMAGNETIC CONVERTER

It is based on the Faraday-Neumann-Lenz law, according to which, a time-variable magnetic flux and voltage are generated due to the relative motion between a coil and a permanent magnet [29], [32], [34], as shown in Fig. 6. The amount of electricity generated depends on the strength of the magnetic field, velocity of the relative motion and the number of turns on the coil.

A comparative analysis of these converters is presented in Table 1 [1], [3], [29]. It is observed that although piezoelectric converters produce the highest voltage and

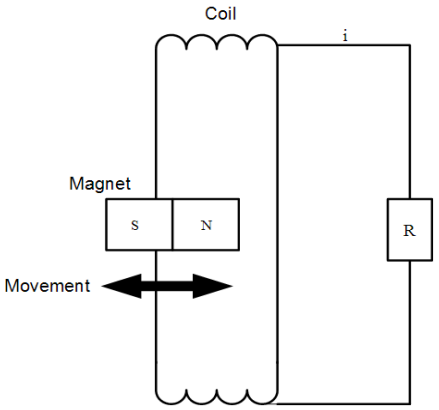

FIGURE 6. Electromagnetic mechanical-to-electrical converter concept model.

TABLE 1. Comparative analysis of different vibration based harvesters.

Feature	Piezoelectric	Electrostatic	Electromagnetic
Output Voltage	High voltage (2-10V)	High voltage (2-10V)	Low voltage (< 1V)
MEMS Implementation	Difficult to integrate	Compatible and easy to integrate	Hard to fabricate at micro level
External Source	Not required	Required in electret-free converters	Not required
Energy Density	High	Increase with size reduction	Low
Low Frequency Operation	Self-discharge at low frequencies	Suitable for low frequency	Low efficiency at low frequencies
Other Drawbacks	Poor coupling of piezo films at micro scale	Parasitic capacitance losses	Ohmic loss in coils

power, electrostatic harvesters can be preferred for implantable microsystems since they are easy to fabricate and integrate at the MEMS level, compared to electromagnetic and piezoelectric converters. Also, they are more suitable for low frequency applications while providing high output voltage levels. Hence, an electrostatic based harvester has been proposed in this paper for the cardiac and neural implants.

III. ELECTROSTATIC ENERGY HARVESTING

The electrostatic harvesters consists of two conductive plates which are electrically isolated by air, vacuum or dielectric material, and the relative motion between the plates leads to a capacitance variation, and hence the flow of electrical charges. These are classified into two categories viz. electret-free electrostatic converters and electret-based electrostatic converters.

A. ELECTRET-FREE ELECTROSTATIC HARVESTERS

These are passive converters that use many conversion cycles made of charging and discharging of the capacitor, and hence require an external circuit to convert the mechanical energy into electrical. This active external circuit must be synchronized with the capacitance variation so as to provide the appropriate charge cycle on the harvester structure.

1) PRINCIPLE OF CONVERSION

There are two modes of charging the harvester viz., charge-constrained cycle and voltage-constrained cycle, as shown in Fig. 7 [1], [3], [29], [35]. Both conversion cycles begin at maximum capacitance (C_{max}). In charge-constrained conversion, a charge is injected by the external source to polarize it at C_{max}.

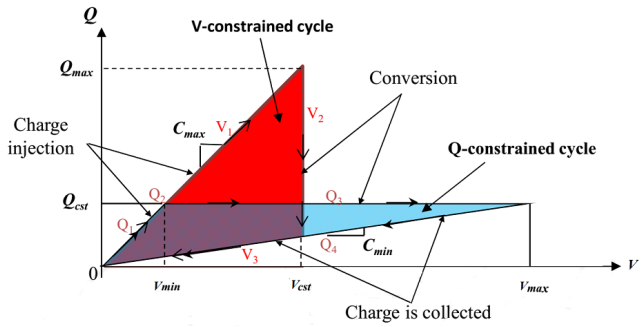

FIGURE 7. Energy conversion cycles of electret-free electrostatic converters [1].

An electric charge Q_{cst} at voltage V_{cst} is stored at the capacitor at this moment. The structure, when open-circuited, starts moving to a position of minimal capacitance (C_{min}) while keeping the charge Q_{cst} constant, which leads to the increase in voltage across the capacitor due to the decrease in the capacitance. At C_{min}, the capacitor reaches at its maximum voltage V_{max} and the electric charges are removed from the structure by connecting the structure to the load, as shown in Fig. 7. This completes one conversion cycle and the total amount of energy converted in each cycle is given by:

$$E_Q = \frac{1}{2} Q_{cst}^2 \left(\frac{1}{C_{\min}} - \frac{1}{C_{\max}} \right) \tag{6}$$

On the other hand, in a voltage-constrained conversion, which also starts initially with maximal capacitance, the structure is polarized by a voltage V_{cst} at C_{max}. In this case, the voltage is kept constant, and with decreasing capacitance due to mechanical motion, the charge on the capacitor increases thereby generating a current that is scavenged and stored. The plates when disconnected from the voltage source and connected to the load, result in the voltage drop and transfer of the charge from the plates to the load, as shown in Fig. 7. The amount of energy converted per voltage-constrained cycle is given by

$$E_V = V_{cst}^2 \left(C_{\max} - C_{\min} \right) \tag{7}$$

B. ELECTRET-BASED ELECTROSTATIC HARVESTERS

Contrary to the electret-free converters that require an external high voltage polarization source to polarize the capacitor at the beginning of each cycle, the electret-based converters use the electrically charged dielectrics that are in a quasi-permanent electric polarization state (electric charges or diploe polarization). The term 'electret' was coined by Oliver Heavsisde [1] by combining two words electricity (elect) and magnet (et). The electret layers are added to either one or both the plates of the capacitor and are able to polarize the harvesters throughout their lives, thereby enabling the direct mechanical to electrical conversion without any external source. Based on the polarization method, electrets are classified into two categories viz. oriented-dipole electrets and real-charge electrets, as shown in Fig 8. The fabrication procedures of oriented-dipole and real-charge electrets can be studied in [36]–[38].

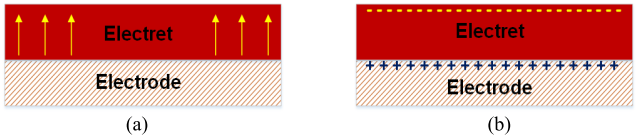

FIGURE 8. Standard electret-based electrostatic converters (a) dipole oriented (b) real-charge electrets.

In accordance with Gauss's law, charge injection or dipole orientation leads to surface potential V_s on the electret and can be expressed as

$$V_s = \frac{\sigma d}{\varepsilon \varepsilon_0} \tag{8}$$

Where, σ is the surface charge density of the electret layer, ε is electret's dielectric permittivity, ε_0 permittivity of vacuum and d is the electret layer thickness. The equivalent model of an electret layer is given in Fig. 9 which consists of a capacitor in series with a voltage source equivalent to the surface voltage of the electret.

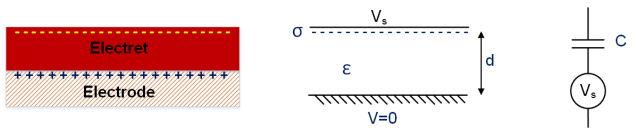

FIGURE 9. Electret layer and its equivalent model.

The capacitance is given by

$$C = \frac{A \varepsilon \varepsilon_0}{d} \tag{9}$$

Where, A is the area of overlap. Some of the materials used as electrets along with their properties are presented in Table 2. As far as implantable microsystems are considered, minimum possible size is the priority. It can be seen from Table 2, that SiO_2 based electrets have minimum thickness while providing highest surface charge densities, along with higher dielectric strength compared to the other electrets.

TABLE 2. Different available electrets and their electrical properties.

Electret Material	Relative Permittivity ϵ	Maximum Thickness	Dielectric Strength (V/μm)	Surface Charge Density (mC/m^2)
Teflon (PTFE/FEP/PFA)	2.1	~100 μm	100-140	0.1-0.25
SiO_2/SiN_3	4/7.5	< 3 μm	500	5-10
Parylene (C/HT)	3	~10 μm	270	0.5-1
CYTOP	2	20 μm	110	1-2
Teflon AF	1.9	20 μm	200	0.1-0.25

Hence, a SiO_2 based electret has been considered in this paper.

1) PRINCIPLE OF CONVERSION

An electret-based electrostatic converter, shown in Fig. 10, is a two plate capacitor structure which consists of a counter electrode (movable electrode) and electret layer over the other electrode. In accordance with the Gauss's law, the electret layer induces charges on electrodes and counter electrodes i.e., if charge on electret layer is Q_e, Q_1 the charge on electrode and Q_2 on counter electrode, then

$$Q_e = Q_1 + Q_2 \tag{10}$$

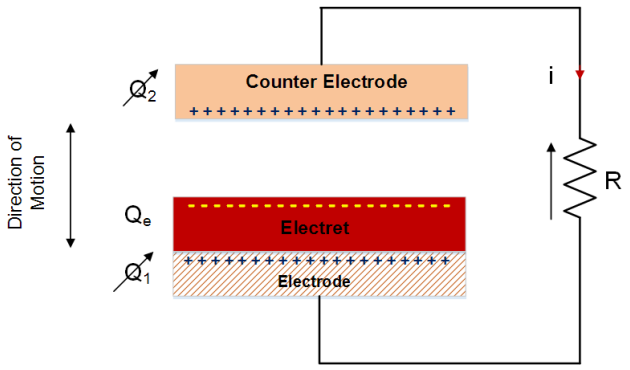

FIGURE 10. Electret-based Electrostatic converter concept model.

On facing the mechanical vibrations, the counter electrode moves towards/away from the electret and the electrode, thereby varying the gap and effect of the electret layer over the counter electrode. This change in the capacitor geometry due to the relative motion leads to reorganization of charges between the electrode and counter electrode via the load resistance as shown in Fig. 11 and hence the current circulation through the resistance. In this manner, a part of mechanical energy is converted into electrical energy by the electret-based electrostatic converter.

The equivalent model of this converter is ideally a voltage source in series with a variable capacitor as shown in Fig. 12(a) [1]. The current flowing through the converter in this case follows the following differential equation

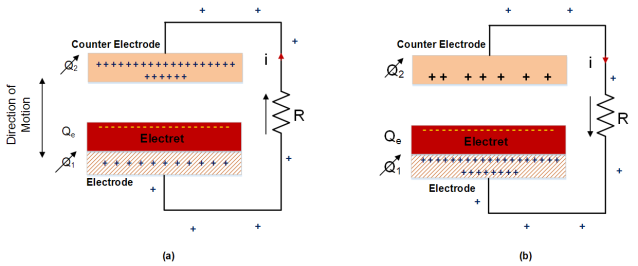

FIGURE 11. Illustration of charge circulation process in Electret-based Electrostatic converter.

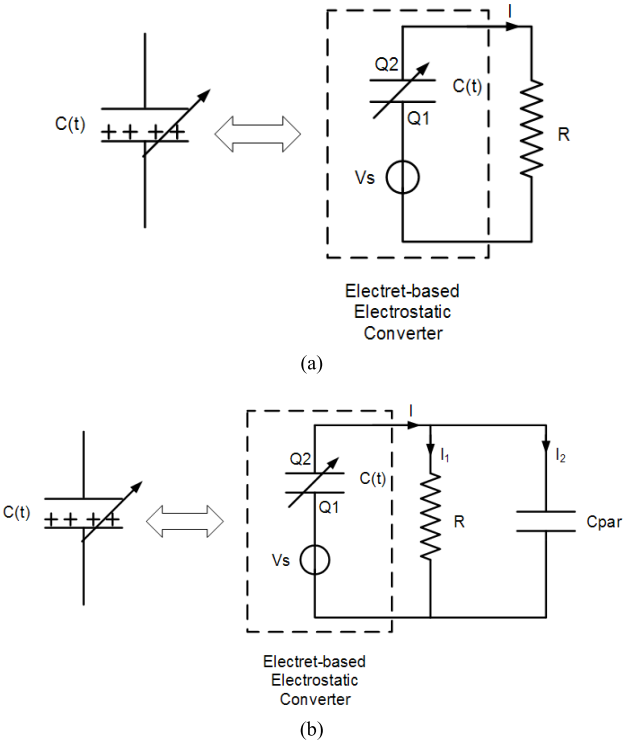

FIGURE 12. Equivalent model of (a) ideal electret-based electrostatic converter and (b) practical electret-based converter with parasitic capacitance.

$$\frac{dQ_2}{dt} = \frac{V_s}{R} - \frac{Q_2}{C(t)R} \tag{11}$$

However, the capacitance generated by the electrostatic converter is quite low. Hence, it is important to include the effect of parasitic capacitance on the structure. The equivalent model in this case is shown in Fig 12(b) [1] and consists of an additional parasitic capacitor in parallel with the converter. The differential equation then gets modified as [1], [39]

$$\frac{dQ_2}{dt} = \frac{1}{\left(1 + \frac{C_{par}}{C(t)}\right)}\left(\frac{V_s}{R} - Q_2\left(\frac{1}{RC(t)} - \frac{C_{par}}{C^2(t)}\frac{dC(t)}{dt}\right)\right) \tag{12}$$

The power generated by the electret-based electrostatic converter is directly proportional to the variation in capacitance due to the external mechanical vibrations and the surface voltage of the electret material used, and is given as [40]

$$P \propto V_s^2 \frac{dC}{dt} \tag{13}$$

IV. DIFFERENT ELECTROSTATIC HARVESTER TOPOLOGIES

The electrostatic transduction mechanism, as already discussed, is a variable capacitor whose capacitance varies with the mechanical displacement and in order to achieve maximum amount of harvested energy, and the capacitance variation needs to be as large as possible. There are various topologies for the MEMS electrostatic devices which differ in terms of the plane of motion and the actuation direction. These topologies can be used in both electret-free and electret-based electrostatic converters. In this section, the description of each structure along with their capacitance values and electrostatics forces is discussed. The capacitance values are calculated using simple plane capacitor model having an electret layer shown in Fig. 13. To use it as an electret-free structure the thickness of the electret layer has to be reduced to zero (d=0). The total capacitance of the single electrode structure of the converter is the series combination of two capacitances C_1 and C_2, and is given by

$$C(t) = \frac{C_1(t)C_2}{C_1(t) + C_2} = \frac{A(t)\varepsilon_0}{g(t) + d/\varepsilon} \tag{14}$$

Where, $C_1(t) = \frac{A(t)\varepsilon_0}{g(t)}$ and $C_2 = \frac{A(t)\varepsilon\varepsilon_0}{d}$

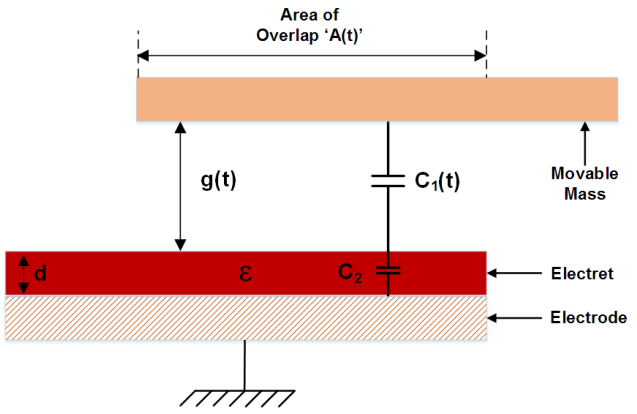

FIGURE 13. Generalized capacitance model of an electret based simple plane converter.

The electrostatic force induced is given by

$$F_{elec} = \frac{d}{dx}(W_{elec}) = \frac{d}{dx}\left(\frac{1}{2}C(x)V_c(x)^2\right) = \frac{d}{dx}\left(\frac{Q_c^2(x)}{2C(x)}\right) \tag{15}$$

Where, W_{elec} is the total amount of energy stored, Q_c is the charge and $V_c(x)$ is the voltage across capacitor C(x)

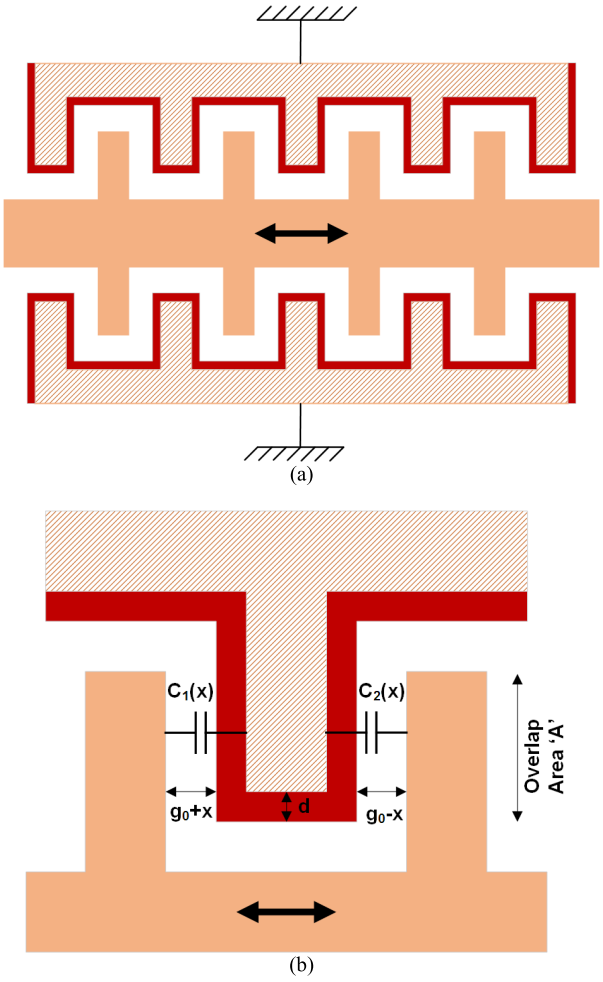

FIGURE 14. (a) Generalized structure of an electret-based in-plane gap closing electrostatic converter (b) close view of capacitances between two electrode fingers of the harvester.

A. IN-PLANE GAP CLOSING CONVERTER

In this structure, the electrodes are inter-digitated as shown in Fig. 14, and due to the external mechanical vibrations there is a variable in-plane gap closing between the fingers, which lead to the capacitance variation. The capacitance of the single electrode element is equal to the parallel combination of capacitances $C_1(x)$ and $C_2(x)$ and is given as

$$C_1(x) = \frac{A\varepsilon_0}{g_0 + d/\varepsilon + x} \tag{16}$$

$$C_2(x) = \frac{A\varepsilon_0}{g_0 + d/\varepsilon - x} \tag{17}$$

$$C(x) = N[C_1(x)||C_2(x)] = \frac{2NA\varepsilon_0(g_0 + d/\varepsilon)}{(g_0 + d/\varepsilon)^2 - x^2} \tag{18}$$

Here, N is the number of electrodes in the entire harvester structure, g_0 is the initial gap between the fingers and A is the area of overlap between finger edge and the movable mass (fixed electrode).

The electric force F_{elec} for charge constrained cycle is give as

$$F_{elec} = \frac{Q_{cst}^2 x}{2\varepsilon_0 N\,(g_0 + d/\varepsilon)\,A} \tag{19}$$

And for the voltage-constrained cycle, it is given as

$$F_{elec} = \frac{2V_{cst}^2 x \varepsilon_0 NA\,(g_0 + d/\varepsilon)}{\left((g_0 + d/\varepsilon)^2 - x^2\right)^2} \tag{20}$$

B. OUT-OF-PLANE GAP CLOSING CONVERTER

A variation in the gap between the fixed electret layer electrode and movable electrode occurs due to the out of plane motions between these electrodes, as shown in Fig. 15.

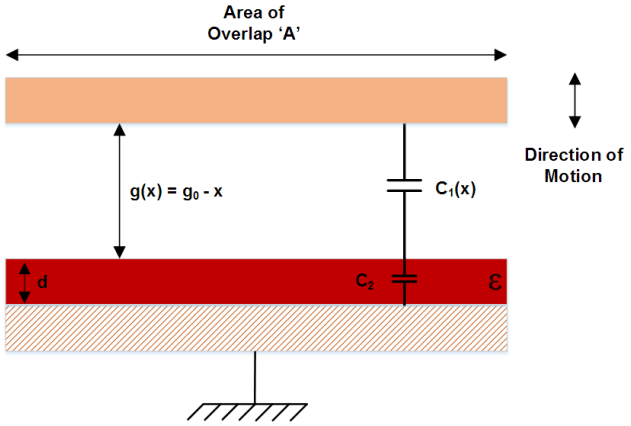

FIGURE 15. Generalized structure of an electret-based out-of-plane gap closing electrode elements.

The capacitance of the single electrode structure is the series combination of the $C_1(t)$ and C_2 capacitances and given as

$$C(x) = N\frac{C_1(x)C_2}{C_1(x) + C_2} = \frac{NA\varepsilon_0}{g_0 + d/\varepsilon - x} \tag{21}$$

Where, $C_1(x) = \frac{A\varepsilon_0}{g_0 - x}$ and $C_2 = \frac{A\varepsilon\varepsilon_0}{d}$

N is the number of electrode elements in the entire harvester structure. The electric force F_{elec} for charge constrained cycle is give as

$$F_{elec} = \frac{Q_{cst}^2 x}{2\varepsilon_0 NA} \tag{22}$$

And for the voltage-constrained cycle, it is given as

$$F_{elec} = \frac{V_{cst}^2 \varepsilon_0 NA}{2\,(g_0 + d/\varepsilon - x)^2} \tag{23}$$

C. IN-PLANE AREA OVERLAP CONVERTER

In this structure, the electrodes are inter-digitated as shown in Fig. 16 and due to the external mechanical vibrations there is a variable in-plane area overlap between the fingers, which leads to the capacitance variation. The whole structure can be viewed as an array of two capacitances C_{E1} and C_{E2}.

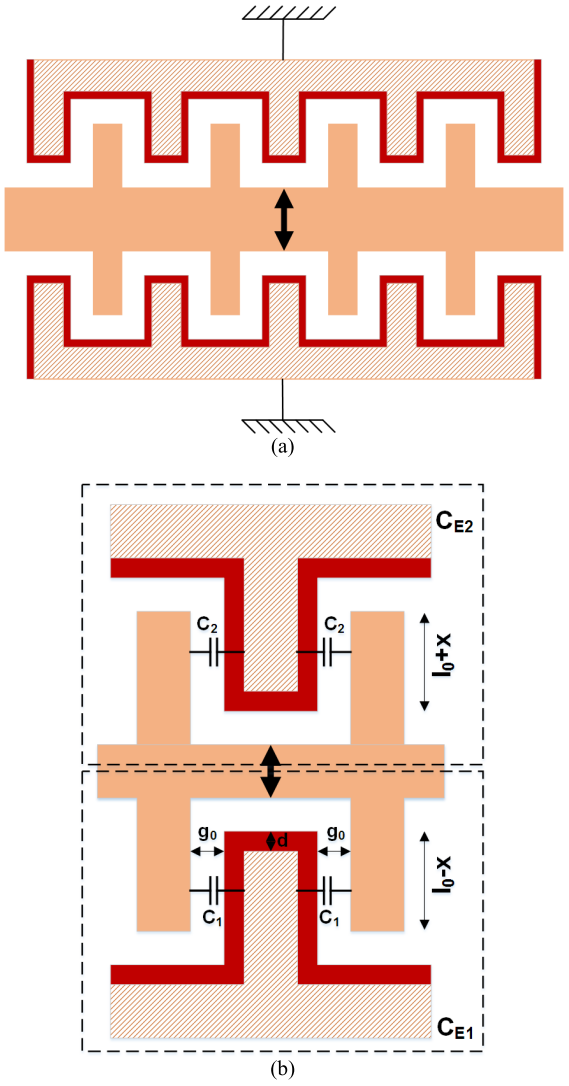

FIGURE 16. (a) Generalized structure of an electret-based in-plane area overlap electrostatic converter (b) close view of capacitances between two electrode fingers of the harvester.

As C_{E1} increases, capacitance C_{E2} decreases and vice versa. These two capacitances are given by

$$C_{E1} = \frac{2N\varepsilon_0 w(l_0 - x)}{g_0 + d/\varepsilon} \tag{24}$$

$$C_{E2} = \frac{2N\varepsilon_0 w(l_0 + x)}{g_0 + d/\varepsilon} \tag{25}$$

The total capacitance on the entire harvester structure is N times the series combination of these two capacitances, where N is the number of electrodes elements.

The electric force F_{elec} for charge constrained cycle in this case is give as

$$F_{elec} = \frac{Q_{cst}^2\,(g_0 + d/\varepsilon)}{2\varepsilon_0 Nw\,(l_0 + x)^2} \tag{26}$$

And for the voltage-constrained cycle, it is given as

$$F_{elec} = \frac{V_{cst}^2 \varepsilon_0 Nw}{2\,(g_0 + d/\varepsilon)} \tag{27}$$

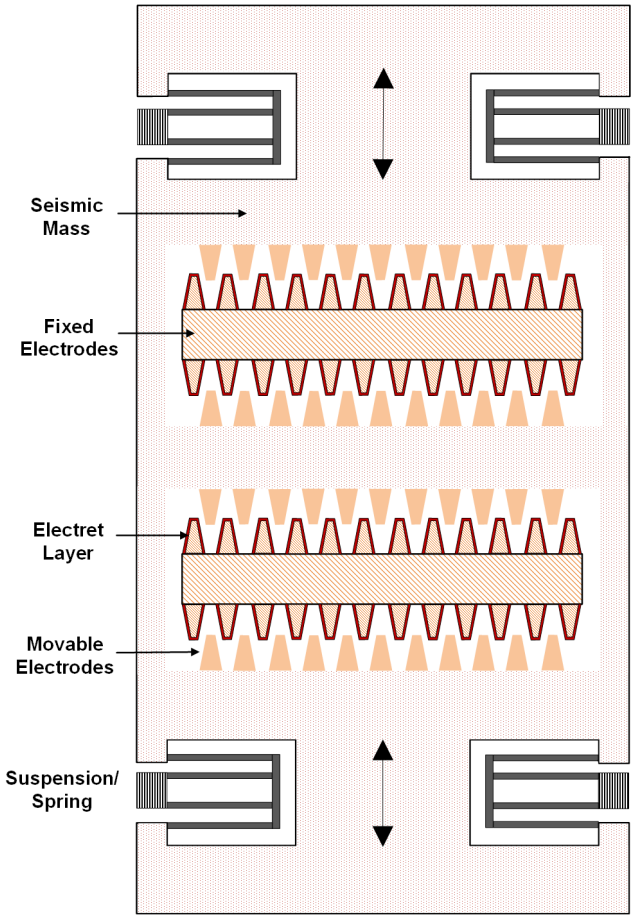

FIGURE 17. Illustration of the proposed electret based electrostatic energy harvester depicting the mobile generator/seismic mass, suspensions/springs and angled electrodes.

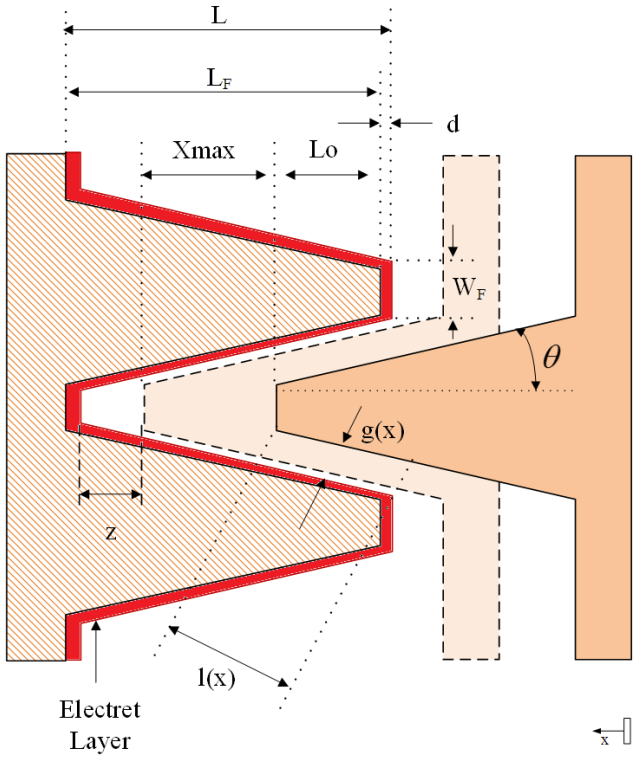

FIGURE 18. Illustration of the structure of the proposed electret based angular electrode.

V. PROPOSED ELECTRET-BASED ANGULAR HARVESTER

The basic electrostatic harvester topologies discussed earlier can be categorized as area-overlap and gap-closing converters [1], [41]–[45]. However, they provide small capacitance variation. Hence, a new electret based electrostatic energy harvester with angular electrodes, shown in Fig. 17, has been proposed which obtains larger capacitance variation with respect to displacement of the generator mass. The operation of this harvester is similar to that of simple electret-based harvester discussed in section III, subsection B.1. One such trapezoidal electrode structure based electret-free harvester has been proposed in [46]. Fig. 18 shows the zoomed view of a single proposed electret based angular electrode structure wherein θ is the angle of the electrodes, L_o the initial electrode fingers overlap length, L is the length of an electrode finger and W_F its width. The capacitance between the inter-digitated electrodes is dependent on the height of the electrode fingers H_F, which is equal to the device layer thickness, gap $g(x)$ between the electrodes and the overlap length $l(x)$. The total capacitance of the proposed harvester consists of two components viz., capacitance due to gap closing of electrode finger tips and capacitance due to gap and area overlap variation.

The capacitance due to gap closing of finger tips, shown in Fig. 19, is given as

$$C_p(x) = 2\frac{C_1(x)\cdot C_2}{C_1(x)+C_2} = \frac{2\varepsilon_0 w_F H_F}{d/\varepsilon + z + (x_{\max} - x)} \quad (28)$$

$$C_1(x) = \frac{\varepsilon_0 w_F H_F}{g} \quad (29)$$

$$C_2 = \frac{\varepsilon\varepsilon_0 w_F H_F}{d} \quad (30)$$

Where, z is the minimum gap between the fingertip and base of the electret layer and ε is the permittiity of the electret.

The gap g(x) between the electrodes is a linear function of displacement x and is given as

$$g(x) = g_{\min} + (x_{\max} - x)\cdot\sin(\theta) \quad (31)$$

Here the minimum gap g_{min} between the electrodes is obtained for maximum displacement $x{=}x_{max}$. The overlap length of the inter-digitated electrodes can be computed as

$$l(x) = \frac{x_{\max} + x}{\cos(\theta)} + g(x)\cdot\tan(\theta) \quad (32)$$

The capacitance for the single inter-digitated electrode element due to area overlap and gap variations, shown

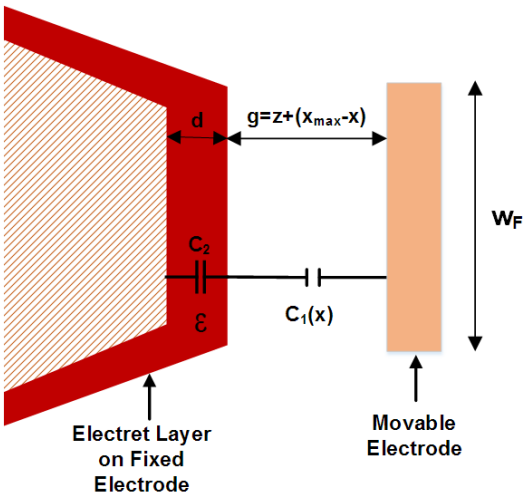

FIGURE 19. Zoomed view of capacitances due to gap closing in the fingertips of the electret based angular electrodes.

in Fig. 20, is given as

$$C_3 = \frac{\varepsilon\varepsilon_0 l(x) H_F}{d} \tag{33}$$

$$C_E(x) = \frac{\varepsilon_0 l(x) H_F}{g(x)} \tag{34}$$

$$C_g(x) = 2\frac{C_E(x)\cdot C_3}{C_E(x)+C_3} = \frac{2\varepsilon_0 l(x) H_F}{g(x)+d/\varepsilon} \tag{35}$$

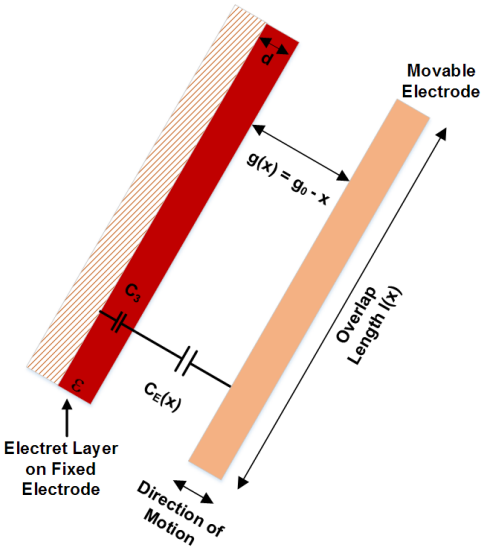

FIGURE 20. Zoomed view of capacitances in the angular sides of the electret based electrodes.

Substituting g(x) and l(x) from equations (31) and (32) into (35), we get the expression of the capacitance variation with respect to the displacement as

$$C_g(x) = \frac{2\varepsilon_0 H_F\left[\frac{x_{\max}+x}{\cos(\theta)} + g(x)\cdot\tan(\theta)\right]}{g(x)+d/\varepsilon} \tag{36}$$

$$C_g(x) = \frac{2\varepsilon_0 H_F\left[x_{\max}+x+g_{\min}\cdot\sin(\theta)+(x_{\max}-x)\cdot\sin^2(\theta)\right]}{\frac{d}{\varepsilon}\cos(\theta)+g_{\min}\cdot\cos(\theta)+(x_{\max}-x)\cdot\sin(\theta)\cos(\theta)} \tag{37}$$

The total capacitance of the proposed electret based energy harvester is given as

$$C_T(x) = N(\theta)\cdot\left[C_g(x)+C_p(x)\right] = N(\theta)C_{SE}(x) \tag{38}$$

Here $C_{SE}(x)$ is the total capacitance of single electrode structure shown in Figure 18 and N(θ), a function of angle θ, is the number of electrode fingers in the proposed harvester, given as

$$N(\theta) = \frac{L_T}{2\left[w_F+(L_f+d)\cdot\tan(\theta)\right]} \tag{39}$$

The maximum capacitance of single electrode element can be computed for maximum displacement and is given as

$$C_{SE}^{\max}(\theta) = 2\varepsilon_0 H_F\left[\frac{2x_{\max}+g_{\min}\cdot\sin(\theta)}{\frac{d}{\varepsilon}\cos(\theta)+g_{\min}\cdot\cos(\theta)} + \frac{w_F}{d/\varepsilon} + z\right] \tag{40}$$

And the total maximum possible capacitance of the proposed electret based harvester can then be computed as

$$C_T^{\max}(\theta) = N^{\max}(\theta)\cdot C_{SE}^{\max}(\theta) \tag{41}$$

The output of the energy harvester is fed to the switching converter shown in Fig. 21, where V_s is the surface potential of the electret, SW1 and SW2 are the switches which are opened during most part of the conversion process. C_{par} is the parasitic capacitance and C_{stor} is the storage capacitor. The cycle begins with both switches open and the vibrating mass at maximum deflection. The capacitance of the variable capacitor C_T is at maximum value (C_T^{max}). SW1 closes and the charge is transferred from the electret surface to the movable electrodes of the capacitor C_T. Then SW1 opens and the deflection of the vibrating mass decreases. When the variable capacitance reaches its minimum (C_T^{min}) at $x = -x_{max}$, the voltage across the capacitor has to increase. Then SW2 closes and the charge moves to the storage capacitor (C_{stor}). The deflection then increases and the next conversion cycle starts again. When the amount of energy on the storage capacitor stays constant, maximum energy is scavenged from the harvester.

VI. RESULTS AND DISCUSSIONS

The minimum gap between the electrodes g_{min} is the distance between the electrodes when displacement is maximum $x = x_{max}$. Based on the fabrication set-up and limitations of [46], the minimum allowable feature size is 2.5 μm, hence the minimum gap g_{min} must be greater than or equal to 2.5 μm. When simulated in MATLAB, from equation (31) it is observed that for $g_{min} \geq$ 2.5 μm, the angle θ must be greater than 5.74° as shown in Fig. 22. The shaded portion highlights the prohibited values of θ. For length (L_F) and width (w_F)

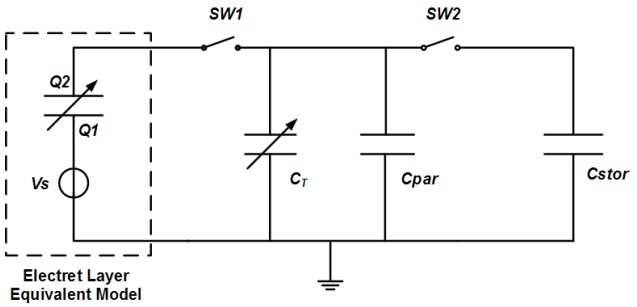

FIGURE 21. Generic model of a switching converter to store the generated charge from the proposed electrostatic converter.

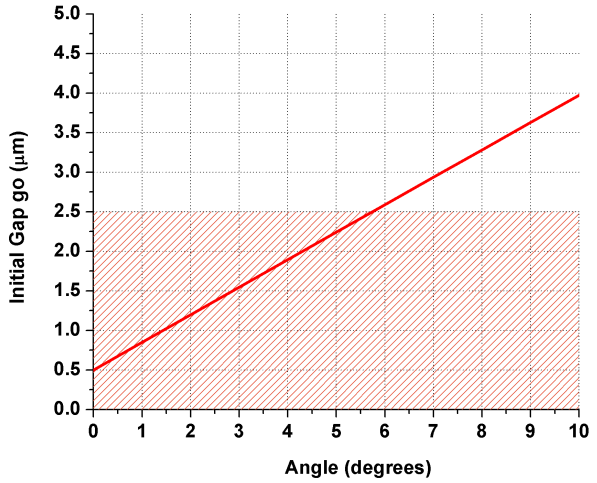

FIGURE 22. Plot of initial gap g_0 with respect to the angle of electrode.

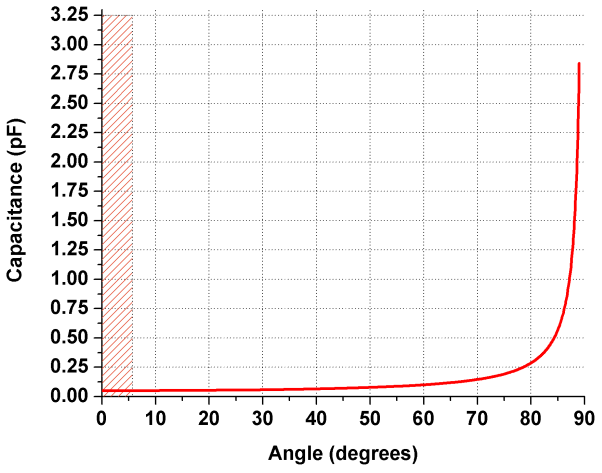

FIGURE 23. Plot of maximum capacitance of a single electrode element of the proposed electret-based converter with respect to the angle of the electrode.

of electrode finger as 45μm and 4μm respectively, and the maximum possible displacement x_{max} of 20 μm, the maximum capacitance of a single electrode structure given in equation (40) increases with increasing value of θ, as shown in Fig. 23 and the overlap length $l(x)$ approaches to

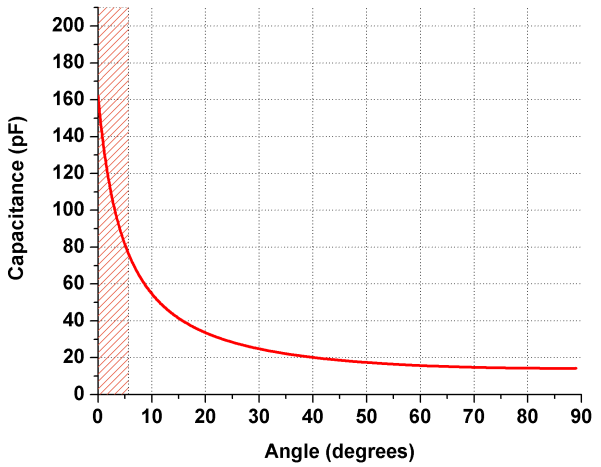

FIGURE 24. Plot of maximum capacitance of the proposed electret-based converter with respect to the angle of the electrode.

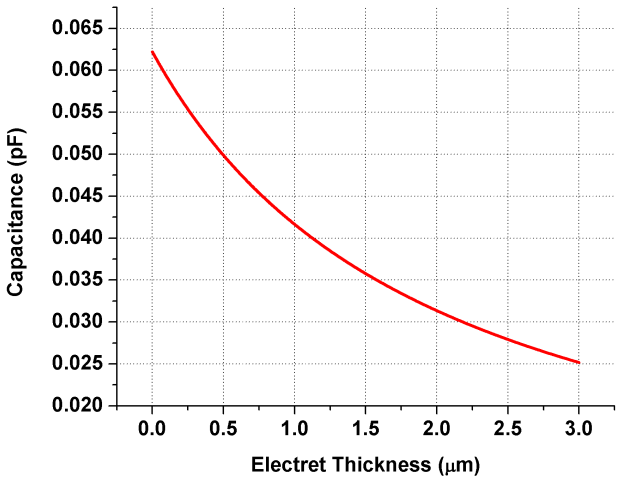

FIGURE 25. Variation of capacitance of a single electrode element with respect to the thickness of the electret layer.

infinity for $\theta = 90°$, however due to the design area limitation, it is not possible. Hence, instead of considering $C_{SE}^{max}(x)$ as the criteria for selecting the value of θ, the variation of maximum total capacitance of the entire structure $C_T^{max}(x)$ at different values of θ is considered.

From Fig. 24 it is observed that the total capacitance decreases with increasing value of θ, hence the minimum possible value of θ i.e. 5.74° is selected as the optimal value of the angle of the electrodes to achieve maximum capacitance variation. Another design parameter to be considered while designing the electret-based harvester is the thickness of the electret layer. The capacitance varies inversely with increasing electret thickness d, as shown in Fig. 25, hence the minimum possible feature size of 0.5 μm is selected as the electret thickness.

After finalizing these design parameters, the capacitance characteristics of a single electrode element $C_{SE}(x)$ and the complete harvester structure $C_T(x)$ was simulated for displacement range of -20 μm to 20 μm at different θ angles

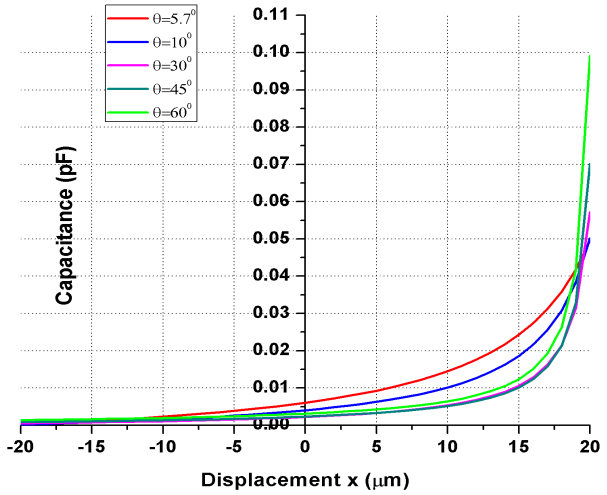

FIGURE 26. Capacitance variation of single electrode element with respect to the displacement due to external vibrations at different angles of electrodes.

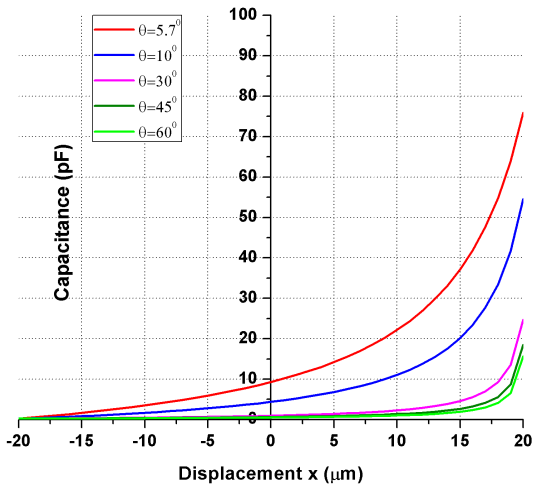

FIGURE 27. Capacitance variation of proposed harvester structure with respect to the displacement due to external vibrations at different angles of electrodes.

and are shown in Fig.26 and Fig. 27 respectively. It is evident that maximum capacitance is obtained when $\theta = 0°$. However, due to the design limitations discussed earlier, this value cannot be considered.

The proposed design thus gives maximum capacitance variation for $\theta = 5.74°$. For the same design specifications, when the proposed electret-based electrostatic harvester is compared with the electret based area-overlap [1] and gap closing harvesters [1], it is evident from Fig. 28 that the proposed harvester provides much better performance and larger capacitance variation. The converter is able is scavenge a maximum power of around 9.6 μW when the proposed active generator, of active layout size 2.5×3.5 mm^2 and volume 0.4375 mm^3, is displaced to a maximum value of $x = x_{max}$, as shown in Fig. 29.

The performance comparison of the harvester with other state-of-the-art electret-based harvesters is presented

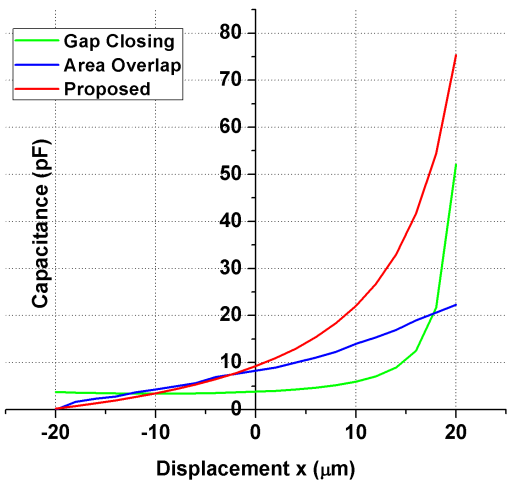

FIGURE 28. Performance comparison of proposed and other electret-based electrostatic converter topologies.

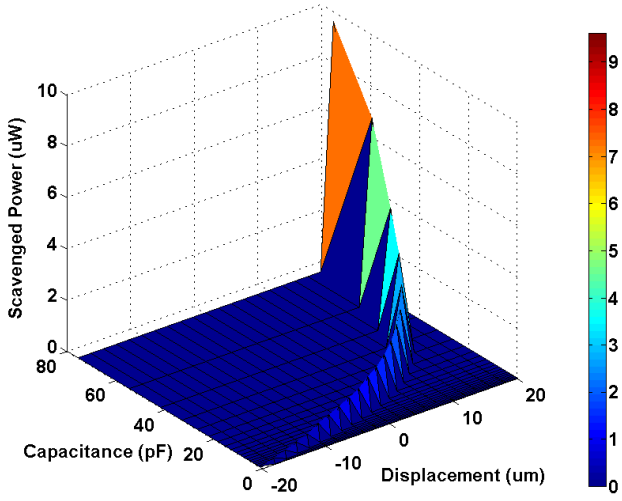

FIGURE 29. Plot of energy generated by the proposed harvester with respect to the displacement and capacitance.

TABLE 3. Comparison of various electret-based electrostatic harvesters.

Harvester	Power (μW)	Area (cm^2)	Power per Unit Area (μW/cm^2)
[2]	20.6	1	20.6
[8]	0.0004616	0.3	0.000154
[9]	40	9	4.44
[16]	4.04	2.34	1.726
Proposed	9.6	0.0875	109.71

in Table 3. It is observed that the proposed electret-based electrostatic harvester with angular electrodes provides highest power per unit area and lies within the maximum limit of power density of 100μW/mm^2 [47], [48] in order to avoid

any damage to the human tissue and can thus be safely used for application in neural and cardiac implants.

VII. CONCLUSION

A SiO_2 electret-based angular electrode structure is designed for incorporation into an electrostatic energy harvester with an aim to provide an alternate energy source to miniaturized cardiac and neural implantable medical devices. Mathematical modeling and analysis showed that the angle θ of the electrodes and the electrode layer thickness d are the important design parameters, constrained by the minimum fabrication feature size available to achieve maximum capacitance variations. The results showed that in comparison to the standard area-overlap and gap-closing topologies, the proposed harvester provides larger capacitance variation with respect to displacement. The output of the harvester structure when fed to the switching converter is able to scavenge energy up to 9.6 μW at maximum displacement. A dc-dc converter can further be applied to generate a regulated voltage from the harvester. Thus the proposed harvester, being small in size of only 2.5×3.5 mm^2 and volume of 0.4375 mm^3 can be used as an energy source for cardiac and neural implants, as they consume power in the range of ∼10 μW.

REFERENCES

[1] S. Boisseau, G. Despesse, and B. A. Seddik, "Electrostatic conversion for vibration energy harvesting," in *Small-Scale Energy Harvesting*. France: InTech, 2012, pp. 91–134.
[2] Y. Chiu and Y.-C. Lee, "Flat and robust out-of-plane vibrational electret energy harvester," *J. Micromech. Microeng.*, vol. 23, no. 1, p. 015012, 2012.
[3] F. U. Khan and M. U. Qadir, "State-of-the-art in vibration-based electrostatic energy harvesting," *J. Micromech. Microeng.*, vol. 26, no. 10, p. 103001, 2016.
[4] J. A. Cramer, "Microelectronic systems for monitoring and enhancing patient compliance with medication regimens," *Drugs*, vol. 49, no. 3, pp. 321–327, 1995.
[5] D.-H. Kim *et al.*, "Epidermal electronics," *Science*, vol. 333, no. 6044, pp. 838–843, 2011.
[6] C. P. Price and L. J. Kricka, "Improving healthcare accessibility through point-of-care technologies," *Clin. Chem.*, vol. 53, no. 9, pp. 1665–1675, Sep. 2007.
[7] S. K. Sia and L. J. Kricka, "Microfluidics and point-of-care testing," *Lab Chip*, vol. 8, no. 12, pp. 1982–1983, 2008.
[8] Z. Yang, J. Wang, and J. Zhang, "A micro power generator using PECVD SiO_2/Si_3N_4 double layer as electret," presented at the PowerMEMS, Sendai, Japan, 2008.
[9] Y. Naruse, N. Matsubara, K. Mabuchi, M. Izumi, and S. Suzuki, "Electrostatic micro power generation from low-frequency vibration such as human motion," *J. Micromech. Microeng.*, vol. 19, no. 9, p. 094002, 2009.
[10] G. Antonioli, F. Baggioni, F. Consiglio, G. Grassi, R. LeBrun, and F. Zanardi, "Stinulatore cardiaco impiantabile con nuova battaria a stato solido al litio," *Minerva Med*, vol. 64, pp. 2298–2305, 1973.
[11] C. F. Holmes, "The role of lithium batteries in modern health care," *J. Power Sour.*, vols. 97–98, pp. 739–741, Jul. 2001.
[12] M. Nathan, "Microbattery technologies for miniaturized implantable medical devices," *Current Pharmaceutical Biotechnol.*, vol. 11, no. 4, pp. 404–410, 2010.
[13] D. C. Bock, A. C. Marschilok, K. J. Takeuchi, and E. S. Takeuchi, "Batteries used to power implantable biomedical devices," *Electrochim. Acta*, vol. 84, pp. 155–164, Dec. 2012.
[14] J. Drews, G. Fehrmann, R. Staub, and R. Wolf, "Primary batteries for implantable pacemakers and defibrillators," *J. Power Sour.*, vol. 97, pp. 747–749, Jul. 2001.
[15] V. S. Mallela, V. Ilankumaran, and N. S. Rao, "Trends in cardiac pacemaker batteries," *Indian pacing Electrophysiol. J.*, vol. 4, no. 4, pp. 201–212, 2004.
[16] Y. Zhang, A. Luo, Y. Xu, T. Wang, A. Zhang, and F. Wang, "Electret-based electrostatic energy harvesting device with the MEMS technology," in *Proc. 12th IEEE/ASME Int. Conf. Mechatron. Embedded Syst. Appl. (MESA)*, Aug. 2016, pp. 1–6.
[17] C. L. Schmidt and P. M. Skarstad, "The future of lithium and lithium-ion batteries in implantable medical devices," *J. Power Sour.*, vol. 97, pp. 742–746, Jul. 2001.
[18] R. Tashiro, N. Kabei, K. Katayama, Y. Ishizuka, F. Tsuboi, and K. Tsuchiya, "Development of an electrostatic generator that harnesses the motion of a living body: Use of a resonant phenomenon," *Int. J. C, Mech. Syst., Mach. Elements Manuf.*, vol. 43, no. 4, pp. 916–922, 2000.
[19] P. Miao, P. D. Mitcheson, A. S. Holmes, E. M. Yeatman, T. C. Green, and B. H. Stark, "MEMS inertial power generators for biomedical applications," *Microsyst. Technol.*, vol. 12, pp. 1079–1083, Sep. 2006.
[20] R. Tashiro, N. Kabei, K. Katayama, E. Tsuboi, and K. Tsuchiya, "Development of an electrostatic generator for a cardiac pacemaker that harnesses the ventricular wall motion," *J. Artif. Organs*, vol. 5, no. 4, pp. 0239–0245, 2002.
[21] V. Leonov, "Thermoelectric energy harvester on the heated human machine," *J. Micromech. Microeng.*, vol. 21, no. 12, p. 125013, 2011.
[22] M. Strasser, R. Aigner, C. Lauterbach, T. Sturm, M. Franosch, and G. Wachutka, "Micromachined CMOS thermoelectric generators as on-chip power supply," *Sens. Actuators A, Phys.*, vol. 114, no. 2, pp. 362–370, 2004.
[23] K. T. Settaluri, H. Lo, and R. J. Ram, "Thin thermoelectric generator system for body energy harvesting," *J. Electron. Mater.*, vol. 41, no. 6, pp. 984–988, 2012.
[24] A. Cuadras, M. Gasulla, and V. Ferrari, "Thermal energy harvesting through pyroelectricity," *Sens. Actuators A, Phys.*, vol. 158, no. 1, pp. 132–139, 2010.
[25] S. R. Hunter, N. V. Lavrik, T. Bannuru, S. Mostafa, S. Rajic, and P. G. Datskos, "Development of MEMS based pyroelectric thermal energy harvesters," in *Proc. SPIE*, vol. 8035, May 2011, pp. 80350V-1–80350V-12.
[26] R. A. Bullen, T. Arnot, J. Lakeman, and F. Walsh, "Biofuel cells and their development," *Biosensors Bioelectron.*, vol. 21, no. 11, pp. 2015–2045, 2006.
[27] K. Dong, B. Jia, C. Yu, W. Dong, F. Du, and H. Liu, "Microbial fuel cell as power supply for implantable medical devices: A novel configuration design for simulating colonic environment," *Biosensors Bioelectron.*, vol. 41, pp. 916–919, Mar. 2013.
[28] N. Mano, F. Mao, and A. Heller, "Characteristics of a miniature compartment-less glucose-O_2 biofuel cell and its operation in a living plant," *J. Amer. Chem. Soc.*, vol. 125, no. 21, pp. 6588–6594, 2003.
[29] S. Koul, S. Ahmed, and V. Kakkar, "A comparative analysis of different vibration based energy harvesting techniques for implantables," in *Proc. Int. Conf. Comput., Commun., Autom. (ICCCA)*, 2015, pp. 979–983.
[30] C. B. Williams and R. B. Yates, "Analysis of a micro-electric generator for microsystems," *Sens. Actuators A, Phys.*, vol. 52, nos. 1–3, pp. 8–11, 1996.
[31] M. Deterre *et al.*, "Micromachined piezoelectric spirals and ultra-compliant packaging for blood pressure energy harvesters powering medical implants," in *Proc. IEEE 26th Int. Conf. Micro Electro Mech. Syst. (MEMS)*, Jan. 2013, pp. 249–252.
[32] A. Khaligh, P. Zeng, and C. Zheng, "Kinetic energy harvesting using piezoelectric and electromagnetic technologies—State of the art," *IEEE Trans. Ind. Electron.*, vol. 57, no. 3, pp. 850–860, Mar. 2010.
[33] S. Chalasani and J. M. Conrad, "A survey of energy harvesting sources for embedded systems," in *Proc. IEEE Southeastcon*, Apr. 2008, pp. 442–447.
[34] S. P. Beeby, M. J. Tudor, and N. M. White, "Energy harvesting vibration sources for microsystems applications," *Meas. Sci. Technol.*, vol. 17, no. 12, p. R175, 2006.
[35] S. Meninger, J. O. Mur-Miranda, R. Amirtharajah, A. Chandrakasan, and J. H. Lang, "Vibration-to-electric energy conversion," *IEEE Trans. Very Large Scale Integr. (VLSI) Syst.*, vol. 9, no. 1, pp. 64–76, Feb. 2001.

[36] T. Onishi, T. Fujita, K. Fujii, K. Kanda, K. Maenaka, and K. Higuchi, "Selective electret charging method of SiO_2 film for energy harvesters by using biased electrode," in *Proc. World Autom. Congr. (WAC)*, 2012, pp. 1–5.
[37] M. Suzuki, M. Shimokizaki, T. Takahashi, Y. Yoshikawa, and S. Aoyagi, "Fabrication and characterization of nano/micro textured electret to avoid electrostatic stiction and enhance its surface potential," in *Proc. J. Phys., Conf.*, 2015, p. 012042.
[38] T. Fujita, T. Toyonaga, K. Nakade, K. Kanda, K. Higuchi, and K. Maenaka, "Selective electret charging method for energy harvesters using biased electrode," *Procedia Eng.*, vol. 5, pp. 774–777, Sep. 2010.
[39] S. Boisseau, G. Despesse, T. Ricart, E. Defay, and A. Sylvestre, "Cantilever-based electret energy harvesters," *Smart Mater. Struct.*, vol. 20, no. 10, p. 105013, 2011.
[40] J. Boland, Y.-H. Chao, Y. Suzuki, and Y. Tai, "Micro electret power generator," in *Proc. IEEE 16th Annu. Int. Conf. Micro Electro Mech. Syst. (MEMS)*, Kyoto, Japan, Jan. 2003, pp. 538–541.
[41] Y. Chiu, C.-T. Kuo, and Y.-S. Chu, "Design and fabrication of a micro electrostatic vibration-to-electricity energy converter," in *Proc. DTIP*, Stresa, Italy, Apr. 2006, pp. 1–6.
[42] R. Guillemet, P. Basset, D. Galayko, and T. Bourouina, "Design optimization of an out-of-plane gap-closing electrostatic vibration energy harvester (VEH) with a limitation on the output voltage," *Analog Integr. Circuits Signal Process.*, vol. 71, no. 1, pp. 39–47, 2012.
[43] D. Hoffmann, B. Folkmer, and Y. Manoli, "Fabrication, characterization and modelling of electrostatic micro-generators," *J. Micromech. Microeng.*, vol. 19, no. 9, p. 094001, 2009.
[44] P. D. Mitcheson, T. C. Green, E. M. Yeatman, and A. S. Holmes, "Architectures for vibration-driven micropower generators," *J. Microelectromech. Syst.*, vol. 13, no. 3, pp. 429–440, Jun. 2004.
[45] Y. Suzuki, "Recent progress in MEMS electret generator for energy harvesting," *IEEJ Trans. Elect. Electron. Eng.*, vol. 6, no. 2, pp. 101–111, 2011.
[46] D. Hoffmann, B. Folkmer, and Y. Manoli, "Analysis and characterization of triangular electrode structures for electrostatic energy harvesting," *J. Micromech. Microeng.*, vol. 21, no. 10, p. 104002, 2011.
[47] A. Ahlbom *et al.*, "Guidelines for limiting exposure to time-varying electric, magnetic, and electromagnetic fields (up to 300 GHz)," *Health Phys.*, vol. 74, no. 4, pp. 494–521, 1998.
[48] *Federal Communications Commission Office of Engineering & Technology*, 4th ed. Washington, DC, USA: OET Bulletin, Aug. 1999, pp. 1–38.

SUHAIB AHMED (S'15) was born in Jammu, India, in 1991. He received the B.E. degree in electronics and communication engineering from the University of Jammu, India, in 2012, and the M.Tech. degree in electronics and communication engineering from Shri Mata Vaishno Devi University, India, in 2014, where he is currently pursuing the Ph.D. degree in electronics and communication engineering.

His research interests include energy harvesting implantable microsystems, data converters, quantum cellular automata, nanotechnology, biomedical signal processing, and the application of wireless sensor networks in health and environment monitoring. He is currently involved in the design and modeling of ultra-low-power mixed signal circuits for submicron devices.

Mr. Ahmed is a member of the International Association of Engineers and an Associate Member of the Universal Association of Computer and Electronics Engineers.

VIPAN KAKKAR (SM'12) was born in Amritsar, India, in 1973. He received the B.E. degree in electronics and communication engineering from Nagpur University, India, in 1994, the M.S. degree from Bradford University, U.K., in 1997, and the Ph.D. degree in electronics and communication engineering from the Delft University of Technology, The Netherlands, in 2002.

He was with Phillips, The Netherlands, as an Engineer and a System Architect from 2001 to 2009, where he was involved in research and development. Since 2009, he has been an Associate Professor with the Department of Electronics and Communication Engineering, Shri Mata Vaishno Devi University, Katra, India. His research interests include nanotechnology, biomedical system and implants design, ultra-low-power analog and mixed signal design, MEMS design, synthesis and optimization of digital circuits, and audio and video processing.

Dr. Kakkar is a Life Member of IETE. He has been an Executive Member of the IEEE, India. He has authored or co-authored many research papers in international conferences and peer-reviewed journals. He has also authored a book on System on Chip Design and has served as an Editorial Board Member of the *Microelectronics Journal* and the *Solid State Electronics* journal.